Amino acid sequences within the β1 domain of human apolipoprotein B can mediate rapid intracellular degradation

Louis R. Lapierre,* Deborah L. Currie,* Zemin Yao,† Jianjun Wang,§ and Roger S. McLeod[1],*

Department of Biochemistry and Molecular Biology,* Dalhousie University, Halifax, Nova Scotia, Canada B3H 1X5; Lipoprotein and Atherosclerosis Research Group,† University of Ottawa Heart Institute, Ottawa, Ontario, Canada K1Y 4E9; and Department of Biochemistry and Molecular Biology,§ Southern Illinois University School of Medicine, Carbondale, IL 62901-4413

Abstract **Apolipoprotein B (apoB)-48 contains a region termed the β1 domain that is predicted to be composed of extensive amphipathic β-strands. Analysis of truncated apoB variants revealed that sequences between the carboxyl termini of apoB-37 and apoB-42 governed the secretion efficiency and intracellular stability of apoB. Although apoB-37, apoB-34, and apoB-29 were stable and secreted efficiently, apoB-42 and apoB-100 were secreted poorly and were degraded by an acetyl-leucyl-leucyl-norleucinal (ALLN)-sensitive pathway. Amino acid sequence analysis suggested that a segment between the carboxyl termini of apoB-38 and apoB-42 was 63% homologous to fatty acid binding proteins (FABPs), which contain orthogonal β-sheets. To test the hypothesis that sequences from the β1 domain are involved in apoB degradation, fusion proteins were created that contained apoB-29 linked to fragments derived from the β1 domain of apoB or to liver FABP. Fusion proteins containing the β1 domain segments apoB-34–42 or apoB-37–42 were degraded rapidly, whereas other fusion proteins were stable and secreted efficiently. Degradation was ALLN-sensitive, and the apoB-34–42 segment increased the association of the apoB protein with the cytosolic surface of the microsomal membrane. Our data suggest that the presence of specific sequences in the β1 domain of human apoB increases degradation by promoting the cytosolic exposure of the protein, although not all regions of the β1 domain are functionally equivalent.**—Lapierre, L. R., D. L. Currie, Z. Yao, J. Wang, and R. S. McLeod. **Amino acid sequences within the β1 domain of human apolipoprotein B can mediate rapid intracellular degradation. *J. Lipid Res.* 2004.** 45: **366–377.**

Supplementary key words endoplasmic reticulum-associated degradation • proteasome • translocation

Apolipoprotein (apo) B is a large and hydrophobic protein that forms the structural backbone for the assembly of triglyceride (TG)-rich lipoproteins (1, 2). Two forms of apoB are found in nature: the full-length apoB-100 (4,536 amino acids) and the truncated apoB-48 (2,152 amino acids), representing the amino-terminal 48% of apoB-100. Both forms are encoded by the same gene, and apoB-48 is the product of an mRNA-editing process (2–4) that generates an in-frame translation termination codon near the middle of the apoB transcript. Despite the difference in polypeptide length, both apoB-100 and apoB-48 contain sufficient sequence information for the assembly and secretion of large TG-rich lipoproteins, suggesting that the ability to recruit neutral lipids during lipoprotein assembly is encoded within the amino-terminal 48% of apoB-100.

The structural elements within the apoB polypeptide that are responsible for lipid recruitment into a lipoprotein particle are poorly characterized. The amino-terminal 670 residues of apoB (∼apoB-15) are disulfide-linked and form a globular domain that is homologous to the primitive lipid transport protein lipovitellin (5) and microsomal triglyceride transfer protein (MTP) (6). However, this region of apoB lacks the ability to recruit substantial quantities of neutral lipid (7). The remainder of the apoB polypeptide may form a "belt" that surrounds the lipoprotein (8), such that the length of the polypeptide determines the size of the nascent particle (9–11). Amphipathic α-helix and β-sheet (12) structures are thought to underlie the unique ability of apoB to assemble lipoproteins with a neutral lipid core (containing cholesteryl ester and TG), and amphipathic β-structures have

Manuscript received 6 March 2003 and in revised form 13 August 2003.

Published, JLR Papers in Press, October 27, 2003.
DOI 10.1194/jlr.M300104-JLR200

Abbreviations: ALLN, acetyl-leucyl-leucyl-norleucinal; apoB, apolipoprotein B; ER, endoplasmic reticulum; FABP, fatty acid binding protein; MTP, microsomal triglyceride transfer protein; PDI, protein disulfide isomerase; PNS, post-nuclear supernatant; PVDF, polyvinylidene difluoride; TG, triglyceride.

[1] To whom correspondence should be addressed.
e-mail: rmcleod2@dal.ca

been identified in both LDL (13) and in model lipid-peptide systems (14).

Predictive algorithms have suggested that the distribution of lipid binding sequences may impart a five-domain structure to human apoB-100 (15) and apoB-100 of other species (16). In this pentapartite model, apoB-48 contains a single large amphipathic β-region (designated the β1 domain) approximately between the carboxyl termini of apoB-22 and apoB-43, flanked by two domains containing amphipathic α-helix (βα1 and α2). Although this working model is used widely for the analysis of apoB structure-function relationships, such a structure has not yet been proven. Working with chimeric proteins, we previously found that multiple short segments within the β1 domain, as few as 150 amino acids, mediate neutral lipid recruitment into VLDL-like lipoproteins (17). Other studies have also suggested a specific role for the β1 domain in TG accretion, particularly sequences between the carboxyl termini of apoB-29 and apoB-41 (18). Carboxyl-terminal truncated mutant forms of apoB are associated with human hypobetalipoproteinemia, a recessive codominant disorder characterized by low concentrations of plasma apoB-containing lipoproteins (19). Characterization of transgenic mice that express truncated human apoB also indicates that the ability of apoB to transport TG is a function of the β1 domain (20).

An important factor that may regulate apoB synthesis and secretion is the intracellular degradation of newly synthesized protein (21). ApoB degradation can occur during and after apoB has translocated across the endoplasmic reticulum (ER) membrane (21, 22) into the lumen of the secretory pathway. In the HepG2 cell, the extent of apoB degradation decreases when exogenous oleic acid is provided, presumably as a consequence of increased lipid biosynthesis (23–25). The coordinated addition of lipids to the apoB polypeptide during VLDL assembly may compete with the degradation processes and thereby determine the level of VLDL secretion (26). Proteasomal degradation of apoB may play a regulatory role in the early stages of apoB biosynthesis, but because the proteasome is on the cytosolic side of the ER, either retrograde translocation of the newly synthesized apoB polypeptides or cytosolic exposure of the nascent chains would be required for this degradation mechanism. Consequently, newly synthesized apoB polypeptides may remain in close association with the translocon (27, 28). Amino acid sequences within apoB that confer this prolonged association with the translocon have not been characterized. Because the intracellular stability of apoB was inversely related to the apoB polypeptide length, and only apoB truncation variants longer than apoB-48 could be detected on the cytosolic side of the microsomal membrane, it has been postulated that the arrested apoB translocation is mediated by sequences downstream of apoB-48 (29). However, like the full-length apoB-100, whose degradation can also be blocked by proteasome inhibitors (26, 30–32), some apoB truncation variants could also be stabilized by proteasome inhibition (29). Thus, degradation of short apoB proteins by the proteasome may occur after translocation of the polypeptide.

Although the region(s) within apoB that make the polypeptide susceptible to proteasomal degradation are unclear, some studies have suggested that the β1 domain of apoB reduces the efficiency of translocation across the ER membrane (33), which arrests apoB in a bitopic orientation with respect to the membrane (34). Lipidation of the apoB polypeptide may prevent its degradation by facilitating translocation and/or by coupling translocation to lipoprotein assembly (35). However, translocation arrest may not be the only mechanism responsible for apoB degradation (36–39), and membrane-associated apoB is not always a substrate for proteasomal degradation [as reviewed in ref. (40)]. On the contrary, the membrane-associated apoB may be the direct precursor of the secreted apoB-containing lipoproteins (41). We have shown previously that short amino acid sequences from apoB, which do not cause significant translocation arrest but are sensitive to proteolytic degradation, appear to colocalize with the lipid binding regions (17, 29). In the current work, sequences within the β1 domain were characterized further using truncated and fusion apoB proteins. The present results indicate that proteasomal degradation of apoB is promoted by some sequences from the β1 domain but not by others. Furthermore, fusion of apoB with a known β-sheet protein does not result in an unstable protein. Thus, unique structural features of the apoB β1 domain are involved in the rapid intracellular degradation of apoB proteins.

EXPERIMENTAL PROCEDURES

Materials

Cell culture reagents were supplied by Invitrogen Canada, Inc. Electrophoresis-grade chemicals for PAGE were obtained from Bio-Rad Laboratories. A mixture of [^{35}S]methionine and [^{35}S]cysteine (ProMix®) and protein A Sepharose CL6B were obtained from Amersham Biosciences (Montreal, QC, Canada). Monoclonal antibodies to human apoB (1D1 and 1C4) were gifts from R. Milne and Y. Marcel (Ottawa Heart Institute). The monoclonal antibody to rat apoB was provided by L. Wong (Louisiana State University, New Orleans, LA). Polyclonal antibodies to apoB (which recognized both human and rat apoB) were purchased from Roche Biochemicals (Montreal, QC, Canada) or were produced in house using normal human LDL as an antigen for antibody production in rabbits. The protease inhibitors acetyl-leucyl-leucyl-norleucinal (ALLN) and leupeptin (acetyl-leucyl-leucyl-argininal) were also purchased from Roche Biochemicals. Monoclonal antibody to bovine protein disulfide isomerase (PDI) and a polyclonal antibody to canine calnexin (carboxyl-terminal cytosolic peptide) were from Stressgen Biotechnologies (Victoria, BC, Canada). MG132 (*Z*-leucyl-leucyl-norleucinal) was from Biomol Research Laboratories, Inc. (Plymouth Meeting, PA), and brefeldin A was from Epicentre Technologies (Madison, WI).

Construction of plasmids encoding apoB-29 fusion proteins

For the construction of apoB-29 fusion protein plasmids, pB29 (17) was digested with *Mlu*I, end-filled with Klenow fragment of DNA polymerase, and ligated with a *Not*I linker (New England Biolabs, No. 1045) to generate a modified pB29 vector that was used to assemble fusion constructs. The fusion proteins con-

tained a linker-encoded pentapeptide (Asp-Ala-Ala-Ala-Ala) between apoB-29 and the remaining protein sequence.

ApoB cDNA fragments encoding apoB-34–B37, apoB-37–B42, or apoB-34–B42 were amplified from the human apoB-48 cDNA (42) using Vent® DNA polymerase (New England Biolabs). Rat liver fatty acid binding protein (FABP) cDNA was amplified from McA-RH7777 cell total RNA by RT-PCR using primers designed based on the published cDNA sequence (43). The 5′ end and 3′ end primers included a *Not*I site and a *Cla*I site, respectively. The PCR product and the pB29 plasmid were digested with *Not*I and *Cla*I and ligated. Ligation mixtures were used to transform *Escherichia coli* strain DH5α, and plasmid DNA for McA-RH7777 transfection was purified by cesium chloride ultracentrifugation.

Cell culture and generation of stable McA-RH7777 cell lines

Parental and transfected McA-RH7777 cells were maintained in 10 cm culture dishes (Falcon) with DMEM containing 10% (w/v) FBS and 10% (w/v) horse serum. For stable cell lines, 200 μg/ml Geneticin was added for selection and maintenance. Stable cell lines were generated using the calcium precipitation technique (11). Cell lines expressing apoB-29, apoB-34, apoB-37, apoB-42, or human apoA-I have been characterized previously (17).

Immunoblot analysis of recombinant human apolipoproteins

The apolipoproteins in total or fractionated medium were concentrated on fumed silica (Sigma-Aldrich), eluted into SDS-PAGE sample buffer, and resolved by PAGE (3–15% gradient gel). Proteins were transferred onto polyvinylidene difluoride (PVDF) membranes by electroblotting (10), and human apolipoproteins were detected using monoclonal antibodies. Anti-mouse immunoglobulin antibodies (labeled with horseradish peroxidase) and enhanced chemiluminescence (Amersham Biosciences) were used to detect the presence of immune complexes on the membrane, according to the manufacturer's recommendations. The liver FABP moiety in the apoB-29/FABP fusion protein was detected using a rabbit polyclonal antibody (a gift of J. Storch, Rutgers University, New Brunswick, NJ).

Metabolic labeling studies of recombinant apolipoproteins

Cells were plated on 60 mm culture dishes (Falcon Primaria®) and grown to 50–70% confluence. The medium was removed and replaced with 1 ml of serum-free and methionine/cysteine-free DMEM containing [^{35}S]ProMix® (200 μCi/ml). After a 60 min pulse, the labeling medium was removed and replaced with chase medium (DMEM). Where indicated, the pulse and chase media were supplemented with FBS (20%, v/v), sodium oleate (0.4 mM), MG132 (25 μM), or ALLN (100 μM). At each time point of the chase, medium was collected and cells were recovered by detergent lysis. In some experiments, cells were permeabilized with digitonin (75 μg/ml) and treated with trypsin (100 μg/ml) after pulse labeling as described previously (29) before lysis of the cells. The apolipoproteins were purified by immunoprecipitation and analyzed by SDS-PAGE and fluorography (10). Radioactivity associated with apolipoproteins was semiquantified by scanning densitometry or by liquid scintillation counting after excision and digestion of the corresponding bands from the gels.

Preparation and analysis of microsomes

Cells were grown to confluence in 10 cm culture dishes and treated for 1 h with ALLN (100 μM), brefeldin A (5 μg/ml), ALLN plus brefeldin A, or vehicle control in DMEM/20% FBS. The monolayers were washed and collected in ice-cold PBS using a cell scraper. After low-speed centrifugation (4 min, 500 *g*), the cells (two dishes per treatment) were suspended in 2 ml of microsome buffer (MSB; 10 mM Tris-HCl, pH 7.4, and 250 mM sucrose) with protease inhibitors [leupeptin (100 μM), PMSF (100 μM), aprotinin (10 kallikrein inhibitor units/ml), ALLN (100 μM)] and disrupted by 20 passes through a ball-bearing homogenizer (H and Y Enterprise, Redwood City, CA). Postnuclear supernatants (PNSs) were prepared by centrifugation of the homogenate at 10,000 *g* for 10 min in an SS-34 rotor at 4°C. Intact microsomes were recovered in the pellet after a 16 min, 100,000 rpm centrifugation in a TLA-100.4 rotor. Protease protection analysis of microsomes was performed as previously described (29), and the proteins were resolved by 3–15% gradient SDS-PAGE and revealed by immunoblotting.

To separate the lumenal content from the microsomal membranes, PNSs were brought to 100 mM sodium carbonate (pH 11) and rotated end-over-end for 30 min at room temperature and then placed on ice. The membranes were recovered by 16 min of centrifugation at 100,000 rpm and 4°C in a TLA-100.4 rotor. The supernatant (containing cytosol and lumenal contents) was removed and neutralized by the addition of 25 μl of 2.5 N HCl. The membrane pellet was resuspended in MSB and brought to 1% SDS, and proteins were solubilized by heating to 75°C for 15 min. An aliquot of the membrane and lumen samples was used to detect PDI and calnexin by Western blot analysis. The remainder of each sample was diluted 10-fold to reduce the SDS content to 0.1%, and apoB was recovered by immunoprecipitation as described above.

ApoB immunoprecipitates were resolved by SDS-PAGE (5% gel), transferred to PVDF membranes, and probed for human apoB using antibody 1D1. Samples of lumenal content and membrane proteins (before immunoprecipitation) were resolved on SDS-PAGE (10% gel), transferred to PVDF membranes, and probed sequentially for PDI and calnexin using the appropriate antibody.

Analytical methods

SDS-PAGE was performed as described by Laemmli (44). Cell protein was quantified according to Bradford (45) using BSA as a standard. Statistical significance was determined using Student's *t*-test.

RESULTS

Secretion and stability of truncated human apoB proteins

To locate sequence elements within the β1 domain that are important for degradation, we compared a series of carboxyl-terminally truncated human apoB proteins, namely apoB-42, apoB-37, apoB-34, and apoB-29 (**Fig. 1A**). McA-RH7777 cells stably expressing human apoA-I were used as a control, in which the secretion of apoA-I was linear and reached 70% efficiency during the 2 h chase (Fig. 1B, open triangles). The secretion efficiency of the truncated apoB (Fig. 1B, closed symbols) varied according to the apoB polypeptide length. Although secretion of apoB-29 was nearly as efficient as that of apoA-I (>50% of initial radiolabel was secreted), the secretion efficiency of apoB-42 was only 20% at the end of the 2 h chase, comparable to that of endogenous apoB-100 (Fig. 1B, open squares).

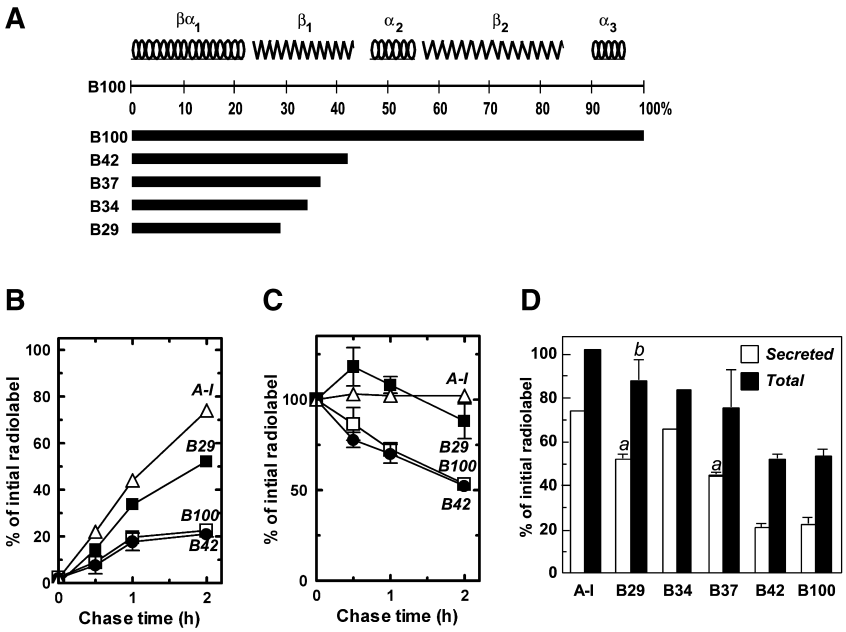

Fig. 1. Secretion and stability of truncated human apolipoprotein B (apoB) proteins in transfected McA-RH7777 cell lines. A: Linear schematic diagram of truncated human apoB proteins. Solid bars represent the apoB coding region relative to the length of apoB-100 (shown on a centile scale). The predicted amphipathic α and β domains are shown on top. B: Secretion of apoB. Transfected cells were pulse-labeled for 30 min with [^{35}S]methionine/cysteine. At the indicated chase time, the apolipoproteins were recovered from the medium by immunoprecipitation, resolved by SDS-PAGE, and visualized by fluorography. Radioactivity associated with each apolipoprotein species was quantified by liquid scintillation counting. Results are expressed as percentages of the initial radiolabel (in the cells at time 0) secreted into the medium. C: Stability of apoB. Cells were pulse-labeled as in B, and the radioactivity associated with both cell and medium apos was combined. Open triangles, human apoA-I (n = 2); closed squares, apoB-29 (n = 3); open squares, apoB-100 (n = 8); closed circles, apoB-42 (n = 3). D: Comparison of truncated apoB secretion and stability. Experiments were performed as described in B. The secretion and stability of apos were determined at the end of a 2 h chase. [a]Significantly different from apoB-100 ($P < 0.001$); [b]significantly different from apoB-100 ($P < 0.05$). In all panels, data points represent means ± SEM, except for apoA-I and apoB34 (mean of duplicates).

Cell-associated apoB and apoA-I radioactivity were also quantified during the chase; the total radioactivity (i.e., the sum of that in cells plus medium) reflected the post-translational stability of the proteins. As shown in Fig. 1C, the recovery of apoA-I was complete during the chase, whereas only ~50% of apoB-100 and apoB-42 were recovered at the end of 2 h of chase, indicative of extensive degradation. In contrast to the instability of apoB-100 and apoB-42, the recovery of apoB-29 was nearly complete, with only ~10% degradation at the end of the 2 h chase. In addition, apoB-34 and apoB-37 were also secreted efficiently and, like apoB-29, were less susceptible to rapid intracellular degradation (Fig. 1D). These observations indicated that secretion efficiency and intracellular stability of the truncated apoB proteins were functions of apoB length between apoB-29 and apoB-42. In addition, a particular region, apoB-37 to apoB-42, was important in determining the fate of apoB (i.e., secretion versus degradation).

Sequence homology between apoB-37 to apoB-42 and FABP

To gain additional insight into the β1 domain structural properties, we searched the protein sequence database (www.ncbi.nlm.nih.gov) using the human apoB-100 sequence as the template. This was performed using the SEQSEE software (46), and the search revealed that, in addition to the known homology between apoB, MTP, and lipovitellin (5), there was significant sequence homology between residues 1,724 to 1,921 of apoB (corresponding to approximately apoB-38.0 to apoB-42.4) and those of FABP family members. A sequence alignment using the XALIGN software (47) indicated that apoB residues 1,724 to 1,921 shared 34% sequence identity and 63% sequence homology with several FABPs of known structure (**Fig. 2**). Interestingly, the alignment of sequences of four mammalian FABPs indicated a level of sequence identity and homology among FABPs similar to that between the apoB fragment and FABP (human, mouse, pig, and rat FABPs have 36.4% identity and 51% homology). Despite sequence variations, structural analysis of all FABP members to date has indicated that they share a common structure, with 10 antiparallel β-strands forming two β-sheets around a central hydrophobic fatty acid binding cavity (48, 49). The X-ray crystal structure of human muscle FABP (Protein Data Bank code: 1hmr) was used as the template to model the apoB fragment using the homology module of

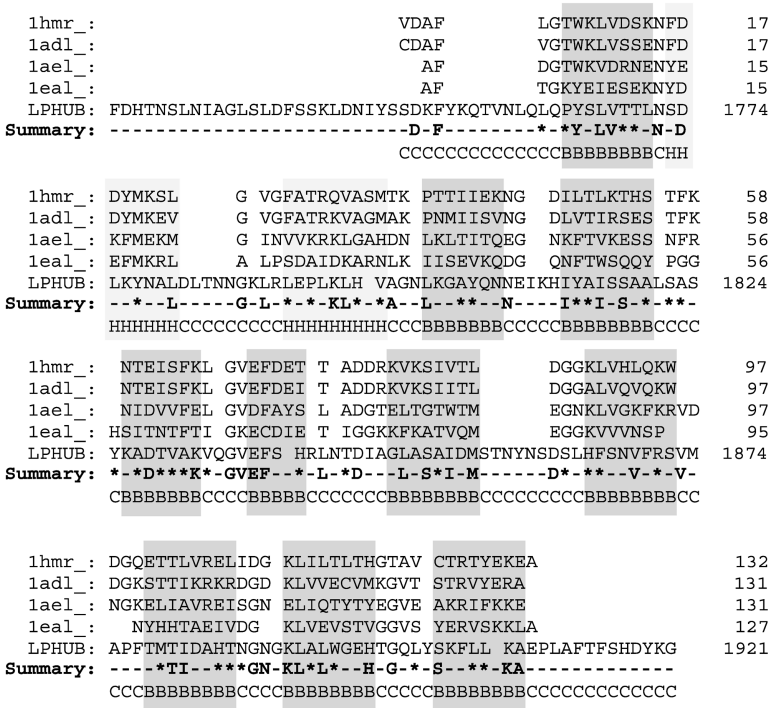

Fig. 2. Sequence alignment of human apoB and fatty acid binding proteins (FABPs). The human apoB (*LPHUB*) amino acid sequence between amino acid residues 1,724 and 1,921 (positions are indicated to the right of each line) was aligned with various FABP sequences. Amino acid identity between apoB and one or more of the FABP sequences (34.1%) is indicated by the single-letter amino acid designation in the summary line. Amino acid homology (63.1%) is indicated by the asterisks in the summary line. The consensus structure is indicated beneath as follows: coil (C), β-sheet (B), or α-helix (H), and β-sheet (dark shading) and α-helix (light shading) regions are indicated as well. FABP family members used for the alignment are as follows: 1hmr_, human muscle FABP; 1adl_, mouse adipocyte lipid binding protein; 1ael_, rat intestine FABP; and 1eal_, pig ileal FABP.

the InsightII software package (Accelrys, San Diego, CA). The model predicted that the secondary structure locations of residues 1,724 to 1,921 of apoB are similar to those of the FABPs, whereas the loop regions in apoB display different lengths (data not shown).

Expression of apoB fusion proteins

We next created apoB fusion proteins that contained segments from either the apoB β1 domain (apoB-29/B-34–37, apoB-29/B-37–42, and apoB-29/B-34–42) or the liver FABP (apoB-29/FABP), in which the amino-terminal 29% of apoB was used as a reporter (**Fig. 3A**). All of the fusion proteins were secreted in a transient transfection assay (Fig. 3B), and using stable cell lines, we compared VLDL assembly, secretion efficiency, and posttranslational stability of the fusion proteins. To determine if the fusion proteins were functional apolipoproteins, sucrose density gradient ultracentrifugation of the culture medium was performed after conditioning with or without exogenous

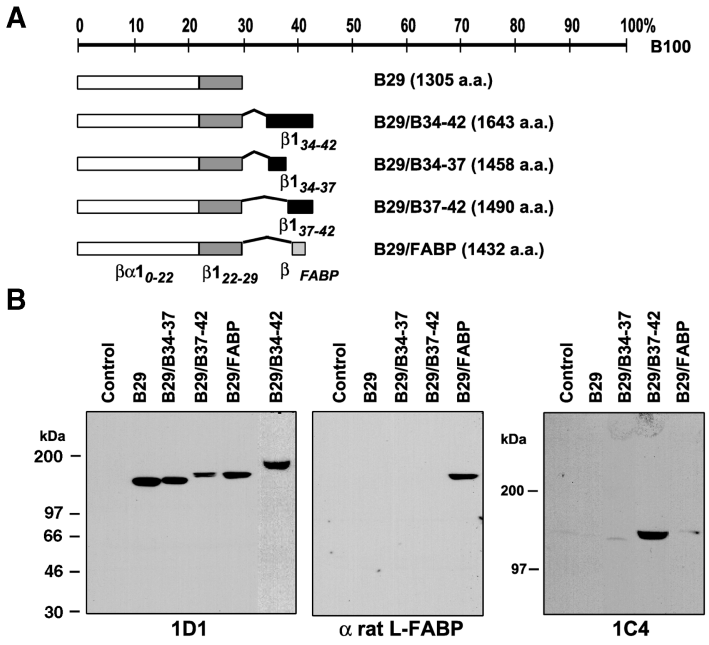

Fig. 3. Construction of apoB fusion proteins. A: Schematic diagrams of apoB-29 fusion proteins. Open bars represent the βα1 region of apoB, corresponding to the amino-terminal 22% of apoB-100. Hatched bars represent the β1 region between the carboxyl termini of apoB-22 and apoB-29. Closed bars represent various sequences from the β1 domain ($\beta1_{34-42}$, $\beta1_{34-37}$, $\beta1_{37-42}$), and the gray bar represents rat liver FABP (β_{FABP}). The length of each fusion protein [in amino acids (a.a.)] is shown in parentheses. B: Immunoblots of apoB fusion proteins transiently expressed in McA-RH7777 cells. The medium was collected at 48 h after transfection, and apoB fusion proteins in the conditioned medium were resolved by SDS-PAGE followed by immunoblot analysis using the indicated antibodies. 1C4 epitope is between the carboxyl termini of apoB-37 and apoB-42.

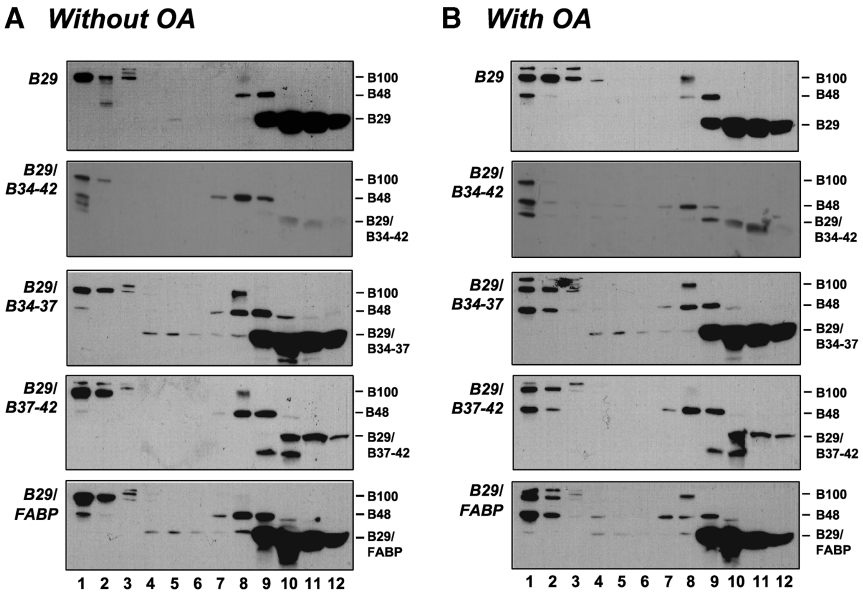

Fig. 4. Density gradient ultracentrifugation of lipoproteins containing apoB fusion proteins. Stably transfected cells (identified to the left of each panel) were incubated for 16–18 h in medium containing 20% FBS without (A) or with (B) oleic acid (OA; 0.4 mM). The conditioned medium was fractionated by ultracentrifugation in a sucrose density gradient. Twelve fractions were collected, and apoB proteins in each fraction were resolved by SDS-PAGE (5% gel) and visualized by Western blot analysis using mixed monoclonal antibodies (1D1 and LRB220). The location of each apoB protein is indicated to the right of each panel. VLDL density corresponds to fractions 1 and 2, and HDL density corresponds to fractions 9–12.

sodium oleate. The apoB-29 was secreted mainly as HDL-like particles (ρ = 1.12–1.21 g/ml, fractions 9–12), regardless of the presence or absence of exogenous oleate (**Fig. 4A**, B, panel *B29*). Fusion protein apoB-29/B-34–42 was secreted as VLDL ($\rho \leq$ 1.02 g/ml, fractions 1 and 2) in addition to HDL-like particles in the presence of exogenous oleate (Fig. 4A, B, panel *B29/B34–42*), suggesting that this protein had the ability to assemble VLDL. However, other apoB fusion proteins (e.g., apoB-29/B-34–37 and apoB-29/B-37–42) and apoB-29/FABP were unable to form VLDL and were secreted primarily as HDL-like particles. In all cell lines, endogenous apoB-48 was secreted as HDL-like particles in the absence of oleate and was secreted as both HDL and VLDL in the presence of oleate. As expected, endogenous apoB-100 was secreted as VLDL whether or not exogenous oleate was added. Thus, short segments from the β1 domain (apoB-34–37 and apoB-37–42) or L-FABP were not sufficient to initiate VLDL assembly, whereas the addition of 8% of apoB sequence from the β1 domain (apoB-34–42) to apoB-29 resulted in a protein that was capable of VLDL assembly.

Pulse-chase analysis of apoB fusion proteins

The low abundance of apoB-29/B-34–42 and apoB-29/B-37–42 in the conditioned medium (Fig. 4) suggested that these fusion proteins may be more susceptible to intracellular degradation than the other fusion proteins. To determine the relationship between posttranslational stability and the β1 domain sequences, we performed pulse-chase analysis on each fusion protein and on the apoB-29 reporter (**Fig. 5**). As shown previously, apoB-29 was efficiently secreted, with >50% recovered in the medium and <30% degraded at the end of a 4 h chase. Thus, apoB-29 may not contain structural elements that mediate rapid posttranslational degradation, even though the protein does contain some β1 domain sequences (between the carboxyl termini of apoB-22 and apoB-29; Fig. 1). The fusion proteins apoB-29/B-34–37 and apoB-29/FABP were also quite efficiently secreted (40–50% of the initial radiolabel), although these two proteins were less stable than apoB-29 (up to 50% degraded). In sharp contrast, almost none of the radiolabeled apoB-29/B-37–42 fusion protein was secreted, and essentially all of the nascent chains were degraded. Similar results were obtained for apoB-29/B-34–42, indicating that apoB-29/B-34–42 was also highly susceptible to degradation. These results suggest that some segments from the β1 domain could alter the secretion and stability characteristics of the apoB-29 reporter and that these changes are not associated with the liver FABP or the apoB-34–37 segment. Furthermore, the most remarkable decreases in stability and secretion were observed in proteins containing the apoB-37–42 segment.

Proteasome inhibition affects the degradation of apoB proteins

The involvement of the proteasome in apoB protein degradation was analyzed using the inhibitors ALLN (100 μM) or MG132 (25 μM). Treatment with ALLN enhanced the stability of endogenous apoB-100 in all of the transfected cell lines by protecting the newly synthesized apoB-

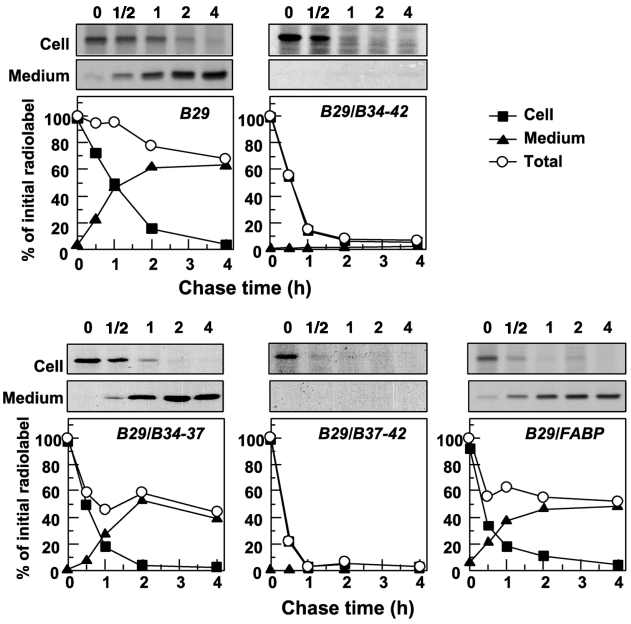

Fig. 5. Pulse-chase analysis of apoB fusion proteins. Stable cell lines were labeled for 1 h with [^{35}S]methionine/cysteine and chased for up to 4 h in DMEM containing 20% FBS, 2 mM methionine, and 0.6 mM cysteine. The apoB fusion proteins in the medium and cells were analyzed by SDS-PAGE and fluorography, and the radioactivity was semiquantified by scanning densitometry. Data are expressed as percentages of the initial radiolabel that was recovered from the cell (closed squares), medium (closed triangles), or cell plus medium (open circles; total). Fluorographs of cell (top panels) and medium (bottom panels) apoB fusion proteins are shown above each graph and are representative of at least three independent experiments.

100 from intracellular degradation (**Fig. 6A**). The total amount of radiolabeled apoB-100 recovered from culture at the end of a 1 h chase increased from ~50% to 70–80%. Secretion of apoB-100 was only modestly increased by the proteasome inhibition (from 11% secreted in the control to 16% secreted with ALLN) (Fig. 6A). Similar increases in stability were observed when cells were treated with MG132, but supplementation of media with exogenous oleate (0.4 mM) had no detectable effect on the stability or the secretion of apoB-100 (data not shown). The stability of apoB-42 (Fig. 6B) was enhanced by proteasome inhibition in a similar manner to apoB-100. The total apoB-42 radiolabel in culture at 1 h of chase increased from ~65% in the absence of inhibitors to ~90% in the presence of ALLN (Fig. 6B). Secretion of apoB-42 was increased by ALLN (from ~15% to ~25–30%), and exogenous oleate had no effect on either the stability or the secretion of this truncated apoB protein (data not shown). The stability of apoB-29 was only marginally affected by ALLN (Fig. 6C), suggesting that the proteasome may not be involved in apoB-29 degradation. The recovery of apoB-29 after a 1 h chase increased from ~85% to 95–100% with proteasome inhibition (Fig. 6C), and neither proteasome inhibition nor exogenous oleate (data not shown) had an effect on apoB-29 secretion. MG132 had a stabilizing effect similar to that of ALLN for apoB-42 but had minimal effect on apoB-29 (data not shown). These observations indicate that apoB-42 and apoB-100 show similar diminished stability and limited secretion resulting from proteasomal degradation, whereas apoB-29 is minimally degraded by the proteasome.

We then examined the characteristics of degradation of the apoB-29 fusion proteins using the proteasome inhibitor ALLN. In the case of apoB-29/B-34–42, treatment with ALLN or MG132 markedly increased apoB-29/B-34–42 stability. Treatment with ALLN markedly increased the recovery of apoB-29/B-34–42 from <10% in untreated cells to 65% in ALLN- treated cells at 1 h of chase (**Fig. 7A**). However, the enhanced stability was not accompanied by increased secretion. Similarly, apoB-29/B-37–42 stability at 1 h of chase increased from <10% to 40% in the presence of ALLN (Fig. 7B). In contrast, ALLN did not appreciably affect the stability of apoB-29/FABP (60–70%; Fig. 7C) or of apoB-29/B-34–37 (data not shown). MG132 treatment of cells gave results that were similar to those obtained using ALLN (data not shown). Thus, the different regions of the apoB β1 domain have different effects on apoB stability, and instability is not induced by fusion of the β-sheet protein FABP to apoB-29.

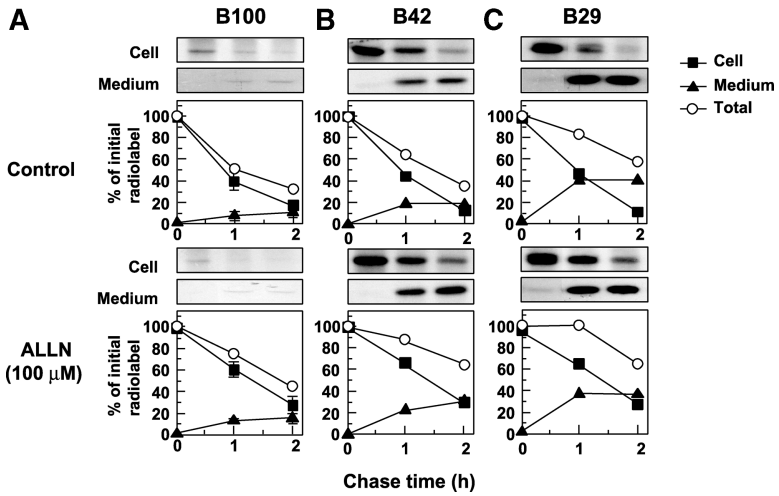

Fig. 6. Effect of proteasome inhibition on the secretion and stability of truncated apoB proteins. Cells expressing apoB-29 (C) or apoB-42 (B) were incubated for 1 h with 100 μM acetyl-leucyl-leucyl-norleucinal (ALLN) or vehicle control, pulse-labeled for 1 h with [^{35}S]methionine/cysteine, and chased for 0, 1, or 2 h under the same conditions. Analysis of apoB proteins was performed as described in the legend to Fig. 5. Error bars in A represent the range of endogenous apoB-100 values in the two cell lines.

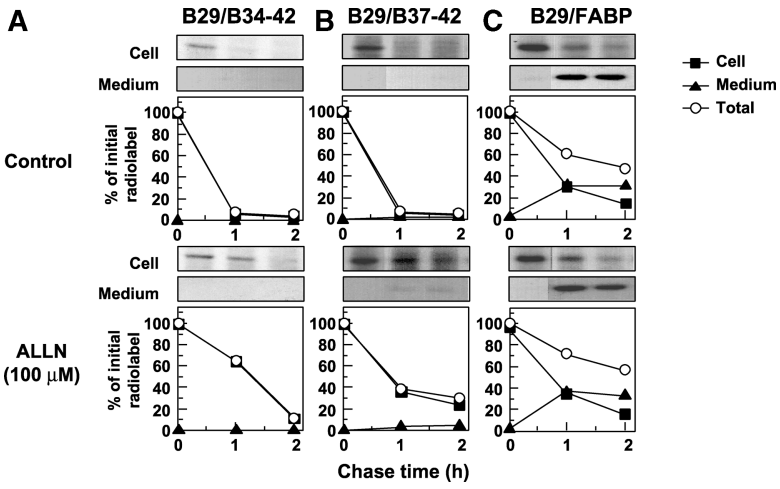

Fig. 7. Effect of proteasome inhibition on the secretion and stability of apoB-29 fusion proteins. Cells expressing apoB-29/B-34–42 (A), apoB-29/B-37–42 (B), or apoB-29/FABP (C) were incubated for 1 h with 100 μM ALLN or vehicle control, pulse-labeled for 1 h with [^{35}S]methionine/cysteine, and chased for 0, 1, or 2 h under the same conditions. Analysis of apoB proteins was performed as described in the legend to Fig. 5.

The presence of the apoB-34–42 segment increases the microsomal membrane association of apoB-29

We hypothesized that the presence of sequences in the β1 domain from beyond apoB-29 (particularly apoB-37–42) may lead to an increase in the association of the protein with the membranes of the secretory pathway and thereby increase exposure to the cytosol. Therefore, we analyzed the distribution of apoB-29, apoB-29/B-34–42, and apoB-42 between microsomal membrane and lumenal content fractions prepared by sodium carbonate extraction of microsomes prepared from cells treated with ALLN (to inhibit proteolytic degradation) and brefeldin A (to block ER exit). Cells were pulse-labeled for 1 h, and microsomal membrane and lumenal content fractions were prepared from a mixture of postnuclear supernatants from all three cell lines. The apoB proteins were then purified by immunoprecipitation and quantified by liquid scintillation counting of the gel bands. The apoB-100 was primarily (88%) associated with the membrane fraction (**Fig. 8A**). In contrast, apoB-29 was found primarily in the lumenal content fraction (35% membrane-associated), and apoB-42 and apoB-29/B-34–42 were equally distributed between the lumen and the membrane (54% and 49% membrane-associated, respectively). This suggested that the presence of the segment of apoB beyond apoB-29 affects the distribution of the apoB proteins and that the apoB-29/B-34–42 fusion protein behaves in a similar manner to the truncated apoB-42. The increased association of the apoB proteins with the membrane may indicate that the proteins were arrested at translocation and exposed to the cytosol.

apoB-34–42 increases the cytosolic exposure of apoB proteins

To examine the topology of the membrane-associated apoB proteins, we analyzed the trypsin sensitivity of apoB-

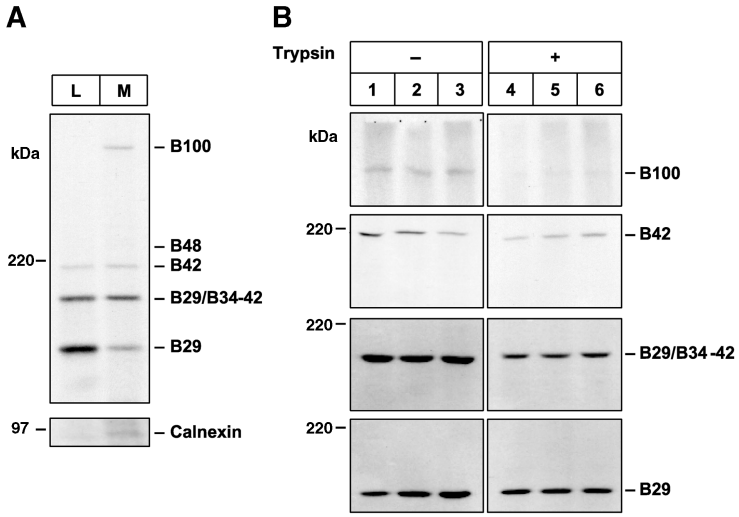

Fig. 8. Analysis of the distribution and topology of nascent apoB proteins in membrane and lumenal contents of microsomes. Cells expressing apoB-29, apoB-29/B-34–42, or apoB-42 were pretreated for 1 h with ALLN (100 μM) and brefeldin A (5 μg/ml) and pulse-labeled for 1 h with [^{35}S]methionine/cysteine in the presence of ALLN and brefeldin A. A: Pooled postnuclear supernatants from cell homogenates were treated with 100 mM sodium carbonate, and the resulting lumenal content (L) and membrane (M) fractions were separated by ultracentrifugation. Lumen and membrane fractions were solubilized separately in 1% SDS, and apoB proteins were precipitated with a polyclonal antibody and visualized by SDS-PAGE with fluorography. B: Cells were labeled for 30 min with [^{35}S]methionine/cysteine and chased with unlabeled amino acids for 15 min in the presence of ALLN and brefeldin A. The cells were then permeabilized with digitonin (75 μg/ml) and incubated in the presence (lanes 4–6) or absence (lanes 1–3) of trypsin (100 μg/ml). After 30 min on ice, the trypsin was inactivated with soybean trypsin inhibitor (500 μg/ml) and the cells were lysed with 1% SDS. The apoB proteins were isolated by immunoprecipitation and visualized by SDS-PAGE with fluorography. Each analysis was performed in triplicate dishes for each cell line.

29, apoB-42, and apoB-29/B-34–42 in digitonin-permeabilized McA-RH7777 cell lines (29). As previously reported (29), apoB-29 was largely protected from exogenous protease (89 ± 3% protected; mean ± SD, n = 3) (Fig. 8B, bottom panels), suggesting that apoB-29 is efficiently translocated (50). In contrast, both apoB-42 and apoB-29/B-34–42 (Fig. 8B) were more sensitive to the added trypsin, as only 41 ± 11% and 53 ± 10%, respectively, of these proteins was protected. ApoB-100 was the least efficiently translocated, as only 15 ± 13% was protected from protease digestion.

In a separate experiment, we also examined the translocation status of each of the model proteins in isolated microsomes (**Fig. 9**). Under the conditions of this analysis, the lumenal PDI was protected from protease degradation but the cytosolic epitope of calnexin was completely degraded (lower panels). The protection of apoB proteins from added protease was essentially identical to that in the permeabilized cell system, as 88 ± 11% of apoB-29 (mean ± SD, n = 5), 68 ± 9% of apoB-42, and 65 ± 16% of apoB-29/B-34–42 were protected from trypsin, as assessed by immunoblot analysis. Consistent with previous observations of the translocation arrest of larger apoB proteins, apoB-100 was no longer detectable in microsomes after trypsin treatment.

These observations suggest that the increase in susceptibility of the apoB proteins to degradation correlates with their level of cytosolic exposure and that this exposure is enhanced by the presence of the fusion of apoB-34–42 to apoB-29.

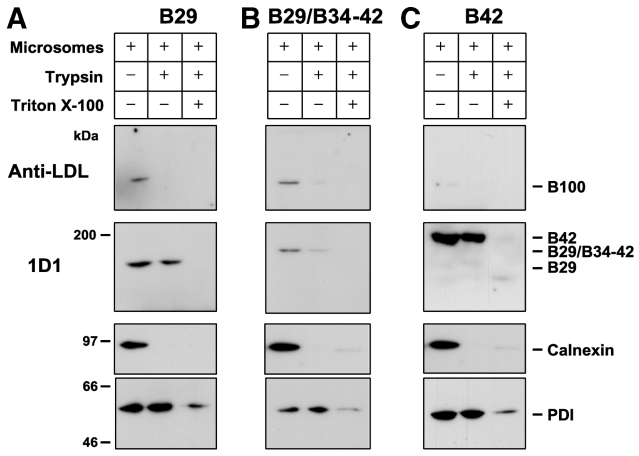

Fig. 9. Immunoblot analysis of the topology of apoB proteins in isolated microsomes. Microsomes were prepared from ALLN- and brefeldin A-treated B29 (A), B29/B34–42 (B), or B42 (C) transfected cells, as described in Experimental Procedures. Aliquots of each microsome preparation were incubated for 30 min on ice in the presence or absence of trypsin (100 μg/ml) and Triton X-100 (1%, w/v) as indicated. Trypsin was inactivated by the addition of soybean trypsin inhibitor (500 μg/ml) and 2% SDS. Proteins were resolved by 3–15% gradient SDS-PAGE and electroblotted to polyvinylidene difluoride membranes. The protection of individual proteins was revealed by immunoblotting for protein disulfide isomerase (PDI), calnexin, human apoB (1D1), or rat apoB (anti-LDL). The migration of molecular mass markers is shown to the left of each panel (kDa), and the protein decorated by each antibody is indicated to the right. Protease protection was quantified by scanning densitometry of representative fluorographs.

DISCUSSION

We have presented evidence that sequences within the β1 domain of apoB can mediate the rapid degradation of apoB proteins. These sequences colocalize with a region that can also mediate core lipid recruitment into VLDL in transfected hepatoma cells. Furthermore, the region implicated shows homology to the FABP family. Comparison of different portions of the apoB β1 domain and of liver FABP fused to apoB-29 indicated that the predicted β-sequences in apoB are not functionally equivalent. Although truncated and fusion proteins containing apoB-37–42 were rapidly degraded in transfected rat hepatoma cells, fusion proteins containing apoB-29 and FABP, a known β-sheet polypeptide, or apoB-34–37 were not. Our findings extend previous observations implicating sequences in the β1 domain in apoB function (33) by suggesting that the susceptibility of apoB proteins to degradation may be related to their ability to form buoyant lipoproteins.

Previous studies (17, 29, 33) and our current work have implicated sequences beyond the carboxyl terminus of apoB-28 in apoB function. Although previous work did not suggest that apoB-48 and apoB-29 were arrested at translocation in rat hepatoma cells (29), model apoB proteins containing only the β1 domain (apoB-42 and novel fusion proteins) were cytosolically exposed in HepG2 cells (33). Our current work indicates that apoB-42 and the apoB-29/B-34–42 fusion protein have a higher affinity for the microsomal bilayer than apoB-29 and are cytosolically exposed. The differences in topology between apoB-42 and apoB-48 in rat hepatoma cells may suggest that apoB-48 has unique properties, perhaps related to sequences between the carboxyl termini of apoB-42 and apoB-48.

Fusion proteins have been useful tools in defining apoB functional sequences in this and other studies. However, one must always be cautious in studies of this type because the model proteins that are used to study structure and function might have properties that are not present in physiologic forms of the protein. Creation of a novel model protein from amino acid sequences that are normally not contiguous in the native protein could introduce functional artifacts associated with misfolding. This is of particular concern in studies of apoB because we have no way of experimentally determining whether the sequences are folded correctly. However, because several of the truncated proteins and fusion proteins that were examined retained the ability to assemble lipoproteins and were quite efficiently secreted, this approach to functional analysis is valid for at least some of the model proteins. One could argue that the proteins that contain the apoB-37–42 region are misfolded in this context and therefore are degraded because they do not retain physiological function. Although we cannot exclude this possibility, at least one of our proteins is able to function in a

manner similar to that of native forms of apoB, in that apoB-29/B-34–42 can assemble VLDL. This observation is consistent with previous observations (18) in which TG recruitment sequences were localized to this region of apoB. In addition, the predicted homology to FABP suggests that sequences within apoB-37–42 may represent a structural or a functional domain. However, conclusive evidence in support of this possibility must await the solution of an apoB structure.

Translocation arrest has been proposed as a mechanism for the cytosolic exposure of apoB during translation, leading to ubiquitination and cotranslational degradation (51). In primary rat hepatocytes (52) and in rat hepatoma cells (53), n-3 fatty acid modulation of apoB degradation was also related to the ability of apoB to recruit lipids. The presence of structures in the β1 domain is believed to be responsible for apoB translocation arrest and subsequent proteasomal degradation (33). A mechanism of extraction of aberrant ubiquitinated apoB from the ER membrane has been proposed, based on studies in HepG2 cells (34). Other evidence has suggested that completely translocated apoB can be destined for degradation in HepG2 and McA-RH7777 cells (17, 36, 54). Moreover, Chan and colleagues (55) demonstrated that the degradation of apoB-100 in HepG2 cells requires targeting of the nascent polypeptide with ubiquitin before translocation into the lumen of the ER for eventual retrograde translocation (28). In the current study, we have demonstrated that sequences downstream of apoB-37 increase the susceptibility of apoB to intracellular degradation, consequently decreasing its secretion. Decreases in stability are found in both the truncated apoB proteins (e.g., apoB-42) and the apoB fusion proteins that contain apoB-29 as the reporter. The marked increase in degradation with the increase in length from apoB-37 to apoB-42 suggests that the sequence between apoB-37 and apoB-42 may play a role in apoB instability, and we have provided evidence that this is related to cytosolic exposure of the protein. The observation that this degradation can be blocked by either ALLN or MG132 implicates the proteasome in a significant portion of the degradation of these apoB proteins. However, because these agents do not prevent all of the degradation of the model proteins, our studies also suggest that other ALLN-insensitive pathways in McA-RH7777 hepatoma cells are involved in the posttranslational degradation of these model apoB proteins, as previously described for apoB-100 in other systems (36, 37).

Our work has identified a significant structural homology between apoB-38.0 and apoB-42.4 and FABP, a well-defined β-sheet protein, providing support for the predicted β-structure of this region of apoB (16, 56, 57). Further development of a model structure based on the homology to FABP may provide additional evidence for a structural relationship between this region of apoB and FABP. However, the analysis of the apoB-29 fusion protein containing FABP suggests that the FABP homology in apoB cannot be functionally replaced by FABP itself.

The studies of intracellular stability and secretion efficiency of the apoB fusion proteins indicate that not all sequences from the β1 domain are involved in apoB degradation. A significant decrease in apoB stability was observed when either the apoB-34–42 or the apoB-37–42 segment was fused to apoB-29, but fusion to apoB-34–37 did not markedly affect secretion or stability and fusion to FABP had little effect on the stability of the resulting model protein. It is also important to note that even apoB-29 contains a portion of the β1 domain but that this protein is not rapidly degraded. This suggests that the instability of apoB is not a function of all regions of the β1 domain and that a proven β-sheet domain does not introduce apoB instability. On the contrary, unique features of the apoB protein sequence, such as the acquisition of the ability to recruit neutral core lipids, may also be associated with translocation arrest and a markedly increased susceptibility to intracellular degradation.

The authors thank Drs. Ross Milne, Yves Marcel, Judith Storch, and Laurence Wong for the gifts of antibodies used in the work. Dr. Khai Tran provided valuable advice in the separation of membrane and lumenal contents of microsomes. This work was supported by grants (to R.S.M.) from the Canadian Institutes of Health Research (42492MOP) and the Heart and Stroke Foundation of Canada (New Brunswick Affiliate).

REFERENCES

1. Davis, R. A. 1999. Cell and molecular biology of the assembly and secretion of apolipoprotein B-containing lipoproteins by the liver. *Biochim. Biophys. Acta.* **1440:** 1–31.
2. Davidson, N. O., and G. S. Shelness. 2000. Apolipoprotein B: mRNA editing, lipoprotein assembly, and presecretory degradation. *Annu. Rev. Nutr.* **20:** 169–193.
3. Powell, L. M., S. C. Wallis, R. J. Pease, Y. H. Edwards, T. J. Knott, and J. Scott. 1987. A novel form of tissue-specific RNA processing produces apolipoprotein-B48 in intestine. *Cell.* **50:** 831–840.
4. Chen, S. H., X. X. Li, W. S. Liao, J. H. Wu, and L. Chan. 1990. RNA editing of apolipoprotein B mRNA. Sequence specificity determined by in vitro coupled transcription editing. *J. Biol. Chem.* **265:** 6811–6816.
5. Mann, C. J., T. A. Anderson, J. Read, S. A. Chester, G. B. Harrison, S. Kochl, P. J. Ritchie, P. Bradbury, F. S. Hussain, J. Amey, B. Vanloo, M. Rosseneu, R. Infante, J. M. Hancock, D. G. Levitt, L. J. Banaszak, J. Scott, and C. C. Shoulders. 1999. The structure of vitellogenin provides a molecular model for the assembly and secretion of atherogenic lipoproteins. *J. Mol. Biol.* **285:** 391–408.
6. Shoulders, C. C., T. M. Narcisi, J. Read, A. Chester, D. J. Brett, J. Scott, T. A. Anderson, D. G. Levitt, and L. J. Banaszak. 1994. The abetalipoproteinemia gene is a member of the vitellogenin family and encodes an alpha-helical domain. *Nat. Struct. Biol.* **1:** 285–286.
7. Herscovitz, H., A. Kritis, I. Talianidis, E. Zanni, V. Zannis, and D. M. Small. 1995. Murine mammary-derived cells secrete the N-terminal 41% of human apolipoprotein B on high density lipoprotein-sized lipoproteins containing a triacylglycerol-rich core. *Proc. Natl. Acad. Sci. USA.* **92:** 659–663.
8. Schumaker, V. N., M. L. Phillips, and J. E. Chatterton. 1994. Apolipoprotein B and low-density lipoprotein structure: implications for biosynthesis of triglyceride-rich lipoproteins. *Adv. Protein Chem.* **45:** 205–248.
9. Spring, D. J., L. W. Chen-Liu, J. E. Chatterton, J. Elovson, and V. N. Schumaker. 1992. Lipoprotein assembly. Apolipoprotein B size determines lipoprotein core circumference. *J. Biol. Chem.* **267:** 14839–14845.
10. Yao, Z. M., B. D. Blackhart, M. F. Linton, S. M. Taylor, S. G. Young, and B. J. McCarthy. 1991. Expression of carboxyl-terminally truncated forms of human apolipoprotein B in rat hepatoma cells. Evidence that the length of apolipoprotein B has a major effect on

the buoyant density of the secreted lipoproteins. *J. Biol. Chem.* **266:** 3300–3308.
11. McLeod, R. S., Y. Zhao, S. L. Selby, J. Westerlund, and Z. Yao. 1994. Carboxyl-terminal truncation impairs lipid recruitment by apolipoprotein B100 but does not affect secretion of the truncated apolipoprotein B-containing lipoproteins. *J. Biol. Chem.* **269:** 2852–2862.
12. Chan, L. 1992. Apolipoprotein B, the major protein component of triglyceride-rich and low density lipoproteins. *J. Biol. Chem.* **267:** 25621–25624.
13. Goormaghtigh, E., V. Cabiaux, J. De Meutter, M. Rosseneu, and J. M. Ruysschaert. 1993. Secondary structure of the particle associating domain of apolipoprotein B-100 in low-density lipoprotein by attenuated total reflection infrared spectroscopy. *Biochemistry.* **32:** 6104–6110.
14. Lins, L., R. Brasseur, M. Rosseneu, C. Y. Yang, D. A. Sparrow, J. T. Sparrow, A. M. Gotto, Jr., and J. M. Ruysschaert. 1994. Structure and orientation of apo B-100 peptides into a lipid bilayer. *J. Protein Chem.* **13:** 77–88.
15. Segrest, J. P., M. K. Jones, H. De Loof, and N. Dashti. 2001. Structure of apolipoprotein B-100 in low density lipoproteins. *J. Lipid Res.* **42:** 1346–1367.
16. Segrest, J. P., M. K. Jones, V. K. Mishra, V. Pierotti, S. H. Young, J. Boren, T. L. Innerarity, and N. Dashti. 1998. Apolipoprotein B-100: conservation of lipid-associating amphipathic secondary structural motifs in nine species of vertebrates. *J. Lipid Res.* **39:** 85–102.
17. McLeod, R. S., Y. Wang, S. Wang, A. Rusinol, P. Links, and Z. Yao. 1996. Apolipoprotein B sequence requirements for hepatic very low density lipoprotein assembly. Evidence that hydrophobic sequences within apolipoprotein B48 mediate lipid recruitment. *J. Biol. Chem.* **271:** 18445–18455.
18. Carraway, M., H. Herscovitz, V. Zannis, and D. M. Small. 2000. Specificity of lipid incorporation is determined by sequences in the N-terminal 37 of apoB. *Biochemistry.* **39:** 9737–9745.
19. Schonfeld, G. 1995. The hypobetalipoproteinemias. *Annu. Rev. Nutr.* **15:** 23–34.
20. Chen, Z., R. L. Fitzgerald, and G. Schonfeld. 2002. Hypobetalipoproteinemic mice with a targeted apolipoprotein (Apo) B-27.6-specifying mutation: in vivo evidence for an important role of amino acids 1254–1744 of ApoB in lipid transport and metabolism of the apoB-containing lipoprotein. *J. Biol. Chem.* **277:** 14135–14145.
21. Fisher, E. A., and H. N. Ginsberg. 2002. Complexity in the secretory pathway: the assembly and secretion of apolipoprotein B-containing lipoproteins. *J. Biol. Chem.* **277:** 17377–17380.
22. Yao, Z., K. Tran, and R. S. McLeod. 1997. Intracellular degradation of newly synthesized apolipoprotein B. *J. Lipid Res.* **38:** 1937–1953.
23. Wu, X., N. Sakata, J. Dixon, and H. N. Ginsberg. 1994. Exogenous VLDL stimulates apolipoprotein B secretion from HepG2 cells by both pre- and post-translational mechanisms. *J. Lipid Res.* **35:** 1200–1210.
24. Tanaka, M., H. Jingami, H. Otani, M. Cho, Y. Ueda, H. Arai, Y. Nagano, T. Doi, M. Yokode, and T. Kita. 1993. Regulation of apolipoprotein B production and secretion in response to the change of intracellular cholesteryl ester contents in rabbit hepatocytes. *J. Biol. Chem.* **268:** 12713–12718.
25. Cianflone, K. M., Z. Yasruel, M. A. Rodriguez, D. Vas, and A. D. Sniderman. 1990. Regulation of apoB secretion from HepG2 cells: evidence for a critical role for cholesteryl ester synthesis in the response to a fatty acid challenge. *J. Lipid Res.* **31:** 2045–2055.
26. Sakata, N., X. Wu, J. L. Dixon, and H. N. Ginsberg. 1993. Proteolysis and lipid-facilitated translocation are distinct but competitive processes that regulate secretion of apolipoprotein B in Hep G2 cells. *J. Biol. Chem.* **268:** 22967–22970.
27. Mitchell, D. M., M. Zhou, R. Pariyarath, H. Wang, J. D. Aitchison, H. N. Ginsberg, and E. A. Fisher. 1998. Apoprotein B100 has a prolonged interaction with the translocon during which its lipidation and translocation change from dependence on the microsomal triglyceride transfer protein to independence. *Proc. Natl. Acad. Sci. USA.* **95:** 14733–14738.
28. Chen, Y., F. Le Caherec, and S. L. Chuck. 1998. Calnexin and other factors that alter translocation affect the rapid binding of ubiquitin to apoB in the Sec61 complex. *J. Biol. Chem.* **273:** 11887–11894.
29. Cavallo, D., R. S. McLeod, D. Rudy, A. Aiton, Z. Yao, and K. Adeli. 1998. Intracellular translocation and stability of apolipoprotein B are inversely proportional to the length of the nascent polypeptide. *J. Biol. Chem.* **273:** 33397–33405.
30. Adeli, K. 1994. Regulated intracellular degradation of apolipoprotein B in semipermeable HepG2 cells. *J. Biol. Chem.* **269:** 9166–9175.
31. Furukawa, S., N. Sakata, H. N. Ginsberg, and J. L. Dixon. 1992. Studies of the sites of intracellular degradation of apolipoprotein B in Hep G2 cells. *J. Biol. Chem.* **267:** 22630–22638.
32. Thrift, R. N., J. Drisko, S. Dueland, J. D. Trawick, and R. A. Davis. 1992. Translocation of apolipoprotein B across the endoplasmic reticulum is blocked in a nonhepatic cell line. *Proc. Natl. Acad. Sci. USA.* **89:** 9161–9165.
33. Liang, J. S., X. Wu, H. Jiang, M. Zhou, H. Yang, P. Angkeow, L. S. Huang, S. L. Sturley, and H. Ginsberg. 1998. Translocation efficiency, susceptibility to proteasomal degradation, and lipid responsiveness of apolipoprotein B are determined by the presence of beta sheet domains. *J. Biol. Chem.* **273:** 35216–35221.
34. Pariyarath, R., H. Wang, J. D. Aitchison, H. N. Ginsberg, W. J. Welch, A. E. Johnson, and E. A. Fisher. 2001. Co-translational interactions of apoprotein B with the ribosome and translocon during lipoprotein assembly or targeting to the proteasome. *J. Biol. Chem.* **276:** 541–550.
35. Boren, J., L. Graham, M. Wettesten, J. Scott, A. White, and S. O. Olofsson. 1992. The assembly and secretion of ApoB 100-containing lipoproteins in Hep G2 cells. ApoB 100 is cotranslationally integrated into lipoproteins. *J. Biol. Chem.* **267:** 9858–9867.
36. Adeli, K., M. Wettesten, L. Asp, A. Mohammadi, J. Macri, and S. O. Olofsson. 1997. Intracellular assembly and degradation of apolipoprotein B-100-containing lipoproteins in digitonin-permeabilized HEP G2 cells. *J. Biol. Chem.* **272:** 5031–5039.
37. Adeli, K., J. Macri, A. Mohammadi, M. Kito, R. Urade, and D. Cavallo. 1997. Apolipoprotein B is intracellularly associated with an ER-60 protease homologue in HepG2 cells. *J. Biol. Chem.* **272:** 22489–22494.
38. Wang, C. N., T. C. Hobman, and D. N. Brindley. 1995. Degradation of apolipoprotein B in cultured rat hepatocytes occurs in a post-endoplasmic reticulum compartment. *J. Biol. Chem.* **270:** 24924–24931.
39. Wu, X., N. Sakata, K. M. Lele, M. Zhou, H. Jiang, and H. N. Ginsberg. 1997. A two-site model for ApoB degradation in HepG2 cells. *J. Biol. Chem.* **272:** 11575–11580.
40. Shelness, G. S., M. F. Ingram, X. F. Huang, and J. A. DeLozier. 1999. Apolipoprotein B in the rough endoplasmic reticulum: translation, translocation and the initiation of lipoprotein assembly. *J. Nutr.* **129:** 456S–462S.
41. Hebbachi, A. M., and G. F. Gibbons. 2001. Microsomal membrane-associated apoB is the direct precursor of secreted VLDL in primary cultures of rat hepatocytes. *J. Lipid Res.* **42:** 1609–1617.
42. Hussain, M. M., Y. Zhao, R. K. Kancha, B. D. Blackhart, and Z. Yao. 1995. Characterization of recombinant human apoB-48-containing lipoproteins in rat hepatoma McA-RH7777 cells transfected with apoB-48 cDNA. Overexpression of apoB-48 decreases synthesis of endogenous apoB-100. *Arterioscler. Thromb. Vasc. Biol.* **15:** 485–494.
43. Gordon, J. I., D. H. Alpers, R. K. Ockner, and A. W. Strauss. 1983. The nucleotide sequence of rat liver fatty acid binding protein mRNA. *J. Biol. Chem.* **258:** 3356–3363.
44. Laemmli, U. K. 1970. Cleavage of structural proteins during the assembly of the head of bacteriophage T4. *Nature.* **227:** 680–685.
45. Bradford, M. M. 1976. A rapid and sensitive method for the quantitation of microgram quantities of protein utilizing the principle of protein-dye binding. *Anal. Biochem.* **72:** 248–254.
46. Wishart, D. S., R. F. Boyko, L. Willard, F. M. Richards, and B. D. Sykes. 1994. SEQSEE: a comprehensive program suite for protein sequence analysis. *Comput. Appl. Biosci.* **10:** 121–132.
47. Wishart, D. S., R. F. Boyko, and B. D. Sykes. 1994. Constrained multiple sequence alignment using XALIGN. *Comput. Appl. Biosci.* **10:** 687–688.
48. Sacchettini, J. C., and J. I. Gordon. 1993. Rat intestinal fatty acid binding protein. A model system for analyzing the forces that can bind fatty acids to proteins. *J. Biol. Chem.* **268:** 18399–18402.
49. Scapin, G., J. I. Gordon, and J. C. Sacchettini. 1992. Refinement of the structure of recombinant rat intestinal fatty acid-binding apoprotein at 1.2-A resolution. *J. Biol. Chem.* **267:** 4253–4269.
50. Macri, J., and K. Adeli. 1997. Studies on intracellular translocation of apolipoprotein B in a permeabilized HepG2 system. *J. Biol. Chem.* **272:** 7328–7337.

51. Pan, M., J. Liang, E. A. Fisher, and H. N. Ginsberg. 2000. Inhibition of translocation of nascent apolipoprotein B across the endoplasmic reticulum membrane is associated with selective inhibition of the synthesis of apolipoprotein B. *J. Biol. Chem.* **275:** 27399–27405.
52. Wang, H., X. Chen, and E. A. Fisher. 1993. N-3 fatty acids stimulate intracellular degradation of apoprotein B in rat hepatocytes. *J. Clin. Invest.* **91:** 1380–1389.
53. Wang, H., Z. Yao, and E. A. Fisher. 1994. The effects of n-3 fatty acids on the secretion of carboxyl-terminally truncated forms of human apoprotein B. *J. Biol. Chem.* **269:** 18514–18520.
54. Huang, X. F., and G. S. Shelness. 1999. Efficient glycosylation site utilization by intracellular apolipoprotein B. Implications for proteasomal degradation. *J. Lipid Res.* **40:** 2212–2222.
55. Liao, W., S. C. Yeung, and L. Chan. 1998. Proteasome-mediated degradation of apolipoprotein B targets both nascent peptides cotranslationally before translocation and full-length apolipoprotein B after translocation into the endoplasmic reticulum. *J. Biol. Chem.* **273:** 27225–27230.
56. Segrest, J. P., M. K. Jones, and N. Dashti. 1999. N-terminal domain of apolipoprotein B has structural homology to lipovitellin and microsomal triglyceride transfer protein. A "lipid pocket" model for self-assembly of apob-containing lipoprotein particles. *J. Lipid Res.* **40:** 1401–1416.
57. Segrest, J. P., M. K. Jones, V. K. Mishra, G. M. Anantharamaiah, and D. W. Garber. 1994. apoB-100 has a pentapartite structure composed of three amphipathic alpha-helical domains alternating with two amphipathic beta-strand domains. Detection by the computer program LOCATE. *Arterioscler. Thromb.* **14:** 1674–1685.